Tariff Schemes and Socioeconomic Factors in Equilibrium Analysis of DER Investments

Miguel Sanchez-Lopez, Andrey Churkin, *Member, IEEE*, Robin Preece, *Senior Member, IEEE*, Rodrigo Moreno, *Member, IEEE*, and Eduardo A. Martinez Ceseña, *Member, IEEE*

***Abstract*—Prosumers' deployment of distributed energy resources (DER) is shaped by market incentives and budget constraints. Effective DER integration can reduce the long-term need for distribution network infrastructure, thereby diminishing overall electricity costs. Nevertheless, it may negatively impact cost allocation among users from different socioeconomic backgrounds. To analyze the efficiency and distributional aspects of DER deployment across different socioeconomic groups, this study employs a novel equilibrium model based on Stackelberg games. The model simulates interactions between a proactive low-voltage distribution network planner and prosumers who may invest in photovoltaic systems and batteries. Prosumers aim to minimize expenses based on tariffs, without knowledge of their peers' decisions. Due to the non-linearities introduced by the tariff structure, a Gauss-Seidel algorithm is employed to reduce model complexity. The study examines six tariff combinations, revealing that cost allocation varies significantly depending on the tariff design. In this regard, the results show the risks associated with certain tariff designs, including potential losses in efficiency or unfair cost allocation. Likewise, the results highlight the value of cost-reflective tariffs in reducing unintended cross-subsidies. These findings underscore the importance of thoughtful tariff design and network planning in promoting both a distributional fairness DER deployment and system-wide efficiency.**

***Index Terms*—Bilevel programming, distributed generation, electricity tariffs, prosumer, Stackelberg games.**

NOMENCLATURE

$\mathcal{I}$	Set of users (i.e., prosumers and consumers)
$\mathcal{T}$	Set of times.
$\mathcal{L}$	Set of lines.
$\mathcal{N}$	Set of nodes.
$\mathcal{K}$	Set of hyperplanes to approximate P-Q feasible area of transmission lines.
A_i^s	Annuity of residential PV panels of user i \$/kW-yr.
$D_{i,t}^A$	Static active demand of user i at time t kW].
$D_{i,t}^R$	Static reactive demand of user i at time t [kVAr].
$\psi_{i,t}^s$	Solar PV generation rate of user i at time t [p.u.].
$\psi_{i,t}^B$	BESS usage rate of user i at time t [p.u.].
K_i	Budget to invest in DER assets of user i [\$].
A_l	Annuity of line l [\$/kW-km-yr].
R_l	Resistance of line l [Ω].
X_l	Reactance of line l [Ω].
$I_{n,l}$	Matrix indicating if line l enters to node n {1,0}.
$O_{n,l}$	Matrix indicating if line l departs from node n {1,0}.
$N_{i,n}$	Matrix indicating if user i belongs to node n {1,0}.
C_t^A	Marginal cost of active energy at time t [\$/kWh].
C_t^R	Marginal cost of reactive energy at time t [\$/kVAr-h].
A_i^B	Annuity of residential BESS of user i [\$/kW-yr].
A_n^R	Annuity of compensator in node n [\$/kVAr-yr].
H_i	BESS energy-to-power ratio [h].
η_i^B	BESS charging efficiency [p.u.].
Δt	Time step [h].

Variables

p_i^s	Solar PV installed capacity by user i [kW].
$e_{i,t}^s$	Solar PV generation by user i at time t [kW].
$e_{i,t}^w$	Active power imports by user i at time t [kW].
$e_{i,t}^{in}$	Active power exports by user i at time t [kW].
$r_{i,t}^w$	Reactive power imports by user i at time t [kVAr].
$r_{i,t}^{in}$	Reactive power exports by user i at time t [kVAr].
$e_{i,t}^{ch}$	Charging power to BESS of user i at time t [kW].
$e_{i,t}^{ds}$	Discharging power from BESS of user i at time t [kW].
p_i^B	BESS inverter capacity of user i [MW].
$SoC_{i,t}$	State of charge of BESS of user i at time t [kWh].

Distribution system variables

s_l	Power capacity of line l [MW].
$p_{l,t}$	Active power in the line l at time t [kW].
$q_{l,t}$	Reactive power in the line l at time t [kVAr].
$i_{l,t}$	Square of the current in the line l at time t [A^2].
$v_{n,t}$	Square of the voltage at node n at time t [V^2].
$c_{n,t}^{in}$	Reactive exports in node n at time t [kVAr].
$c_{n,t}^w$	Reactive imports in node n at time t [kVAr].

Received 4 November 2024; revised 10 April 2025 and 28 July 2025; accepted 8 August 2025. Date of publication 19 August 2025; date of current version 15 December 2025. This work was supported by ANID, Chile, under Grant BECAS/DOCTORADO NACIONAL 21202550, Grant PIA/PUENTE AFB230002, and Grant FONDECYT 1231924. Paper no. TEMPR-00218-2024. *(Corresponding author: Miguel Sanchez-Lopez.)*

Miguel Sanchez-Lopez is with the Department of Electrical and Electronic Engineering, The University of Manchester, M13 9PL Manchester, U.K., also with the Departamento de Ingeniería Eléctrica, Universidad de Chile, Santiago 8320000, Chile, and also with the Instituto Sistemas Complejos de Ingeniería, Santiago 8370397, Chile (e-mail: miguel.sanchezlopez@eng.ox.ac.uk).

Andrey Churkin is with the Dyson School of Design Engineering, Imperial College London, SW7 2DB London, U.K.

Robin Preece is with the Department of Electrical, Electronic Engineering, The University of Manchester, M13 9PL Manchester, U.K.

Rodrigo Moreno is with the Departamento de Ingeniería Eléctrica, Universidad de Chile, Santiago 8320000, Chile, and also with the Instituto Sistemas Complejos de Ingeniería, Santiago 8320000, Chile.

Eduardo A. Martinez Ceseña is with the Department of Electrical, Electronic Engineering, The University of Manchester, M13 9PL Manchester, U.K., and also with the Tyndall Centre for Climate Change Research, M13 9PL Manchester, U.K.

Digital Object Identifier 10.1109/TEMPR.2025.3600063

c_n Reactive compensator capacity in node n [kVAr].
$d^A_{n,t}$ Active demand in node n at time t [kW].
$d^A_{n,t}$ Active demand in node n at time t [kW].
$d^R_{n,t}$ Reactive demand in node n at time t [kVAr].
p^w_t Systemic active imports at time t [kW].
p^{in}_t Systemic active exports at time t [kW].
q^w_t Systemic reactive imports at time t [KVAr].
q^{in}_t Systemic reactive exports at time t [kVAr].

Network linearization
$\widetilde{p}^h_{l,t}$ Active power solution in the line l at time t during iteration h [kW].
$\widetilde{q}^h_{l,t}$ Reactive power solution in the line l at time t during iteration h [kVAr].
$\widetilde{v}^h_{n,t}$ Square of the voltage solution in node n at time t during iteration h [V^2].
α_k Linearization parameter for P-Q feasible area.

Tariff schemes
$\tau^E_{i,t}$ Energy tariff for user i at time t [$/MWh].
$\tau^R_{i,t}$ Reactive energy tariff for user i at time t [$/MVAr-h].
$\tau^D_{i,t}$ Distribution tariff for user i at time t [$/MWh,$/MW].
$\hat{\tau}^D_{i,t}$ Distribution tariff for user i at time t utilized to execute DIM model during Gauss-Seidel algorithm [$/MWh,$/MW].
φ Reduction factor for energy tariff for exports..

I. Introduction

DISTRIBUTED energy resources (DER) play a pivotal role in the decarbonization of the energy sector. DER contribute to decarbonization by enabling the electrification of traditionally non-electric sectors, such as transportation, and by utilizing renewable energy sources for distributed generation. A key characteristic of these resources is that their deployments are decentralized and typically undertaken by consumers or prosumers who respond to economic incentives, with tariffs being the primary economic lever guiding DER development. Studies have also highlighted that socioeconomic factors and budget constraints can significantly influence DER deployment [1], particularly for capital-intensive resources like distributed PV generation and battery equipment. Thus, it is paramount to study the effects of these factors on DER deployments.

The growing integration of DER into electricity distribution networks (DN) presents significant technical and economic challenges. One major concern is that the increased penetration of DER, particularly in distribution networks, can lead to issues such as over voltage, potentially requiring substantial investments in network infrastructure [2]. Nonetheless, with proper planning and management, DER could also alleviate network stress and reduce investment costs by up to 70% [3]. Furthermore, the widespread deployment of DER may disproportionately increase the cost of electricity for consumers without DER installations, as the costs associated with reinforcing DN could be borne by all users, including those who have not adopted DER technologies [4], [5]. This shift challenges the traditional view of electricity as a public good, positioning it increasingly as a marketable commodity [6], [7], and transforming the conventional structure of power systems, where energy flows unidirectionally from generators to demand centers [8].

The challenges associated with DER integration have been widely recognized in academic literature, which examines the effects on prosumers, distribution networks, and upstream power systems. According to [9], local energy markets can be structured in various ways, such as peer-to-peer (P2P) models without a central coordinator, or community-based structures with a coordinating entity, or interconnected community-based markets. In [10], different local energy trading structures are reviewed, ranging from cooperative pricing schemes to non-cooperative frameworks where prosumers interact with a central coordinator and modify their net demand by investing in solar PV or energy storage. A key question is how coordinators can provide effective economic signals to incentivize local market participation, often through tariffs, though subsidies and taxes are also employed.

Research on low-voltage (LV) network congestion due to increased demand and distributed generation highlights the need for further exploration in network modeling and congestion management mechanisms. Equilibrium models based on Stackelberg games (SG) have emerged as a prevalent framework for analyzing local market interactions, both between prosumers and central entities such as distribution system operators (DSOs) [11], [12], [13], [14], [15], [16], [17], [18], [19] and in the context of larger generation and flexibility markets [20], [21], [22], [23], [24], [25]. In the former framework, central entities, often acting as leaders in the game, interacting with prosumers who either have fixed DER capacities or can adjust their installations to reach market equilibrium [13], [14], [18].

In terms of network modeling, different studies show varying levels of complexity. Some equilibrium models simplify network representation, focusing on the broader system effects while neglecting detailed physical network constraints [11], [12], [19], [21], [22], [23], [24]. Other studies incorporate DC power flow models, though these may not accurately capture physical issues such as voltage limits and reactive power management in LV networks [16], [20], [25]. More sophisticated approaches use AC power flow models to account for operational constraints, although the focus remains on fixed network capacities [15], [17], which means that the capacity of the network is not an optimization variable. While research at the transmission level has advanced in addressing these concerns [26], the LV level remains underexplored, especially with regard to the simultaneous expansion of DN and DER capacities in long-term equilibrium models.

In most jurisdictions, tariffs are the primary economic lever for guiding DER development. Studies have established a clear connection between academic models of DER integration and practical regulatory frameworks [9]. However, many developing countries still rely on regulated volumetric tariffs that do not adequately reflect actual DN usage or energy availability,

limiting the efficiency of DER deployment [27]. As a result, understanding the effects of tariff structures on DER integration and the associated social impacts is critical.

The distributional impacts of tariffs, particularly in relation to cost allocation, have gained increasing attention in recent literature. While efficiency has been the focus of most studies, there is a growing need to address the equity implications of different tariff structures. In this line, the authors in [4] provide a comprehensive review on how justice consideration can be included into energy optimization framework. Likewise, research in [6] has highlighted the importance of comparing policies and tariff schemes, while [5] has examined the distributional effects of 11 different tariff structures, though their analysis is limited to historical data and does not account for prosumers' ability to adjust their demand in response to economic signals.

This study adopts a decentralized framework involving a coordinator (e.g., a DSO), prosumers, and consumers. Prosumers determine their DER investments, and the central entity adjusts LV network capacity accordingly, ensuring a long-term equilibrium. Notably, this approach integrates network capacity expansion with AC power flow models, providing a more accurate representation of physical constraints in a decentralized market structure. Additionally, this work evaluates various combinations of energy and distribution tariffs, examining their distributional impacts across socioeconomic groups characterized by different capacities to invest in DER. This enables a nuanced comparison of tariff structures and their long-term effects on DER deployment and distributional aspect through society, advancing beyond previous studies that did not explicitly consider these factors.

Considering the identified gaps in the current literature, the main contributions of this work are:

- A long-term equilibrium model where both network capacity and DER investments are determined through equilibrium conditions. The model incorporates an AC power flow suitable for LV networks, thereby avoiding physically infeasible solutions and, unlike previous formulations, considers the network capacity as part of the equilibrium problem.
- A pioneering study that considers the long-term equilibrium between distribution networks and DER investments takes into account the varying purchasing power of different socioeconomic groups as a factor limiting DER deployment. This study contributes to the field by comparing the impacts of long-term tariffs on both prosumers and network investments. The findings underscore and quantify the crucial role that tariffs play in achieving fair cost allocation across different customer segments, showing how certain tariffs may offer a fair solution without compromising efficiency.

The remainder of this article is structured as follows. Section II describes the investment models. Section III describes the case study and their results. Section IV offers a discussion and analysis of results. Finally, Section V summarizes the main findings and concludes the article.

II. Methodology

This section describes the modeling framework proposed in this article. A high-level overview of the proposed modeling framework is presented in Fig. 1, illustrating the interconnections between inputs, models, and outputs analyzed throughout this paper. Note that the figure highlights the equations involved in each model, as well as the figures that describe specific methodologies.

Thus, a Centralized Planning Model (CPM) that minimizes the total cost of the system, including DN, energy exchanges with the bulk power system and DER investment. The CPM considers idealized conditions where planner has perfect knowledge of all agents, including prosumer budgets, energy demands, and relevant parameters such as investment costs and solar radiation. Thus, the planner centralizes every investment decision on behalf of every agent.

Next, a Decentralized Investment Model (DIM) is introduced, which is an equilibrium model where prosumers invest in DER to minimize their electricity charges. Analogously, the DN is planned considering the prosumer investment. In this equilibrium model, prosumers are subject to tariffs, including energy and distribution network charges. In this regard, the DIM captures more realistic conditions in comparison with the CPM, due to prosumers seeking to minimize their annual expenses without access to information about their peers' decisions. Notably, the DIM features a proactive distribution planner, inspired by the proactive transmission planner [28], who anticipates DER investments made by prosumers based on distribution network investments. This contrasts with a reactive distribution planner, who relies on exogenous forecasts of DER investments independent from the actual distribution network investments. Also, in this paper, the proactive distribution network planner adopts a social perspective, aiming to minimize total system costs.

Thus, while the CPM serves as a benchmark model that provides reference equilibrium conditions, the DIM model provides a tool to support the tariff-setting process led by the regulator, whose social perspective on cost aligns with the formulation proposed here. It is also worth noting that the DIM model can be customised to better capture the role of the DSO.

The proposed resolution algorithm, based on Gauss-Seidel to solve the non-linear formulation through successive linear problems, as well as the tariffs studied, are discussed in detail below.

A. Centralized Planning Model (CPM)

The CPM, (1)–(26) is formulated as a single-level linear programming (LP), aimed at minimizing total system costs. The objective function considers DN costs, DER investments (solar PV and BESS), and energy exchanges with the bulk system. The DN costs are divided into the capacity of the lines and the cost of reactive compensator that can be added to each node.

Equations (2) and (3) denote power balance. Note that PV and BESS do not provide reactive power in this formulation, which aligns with most practical applications. Equation (4) limits capital expenditures in PV and BESS (i.e., budget constraint).

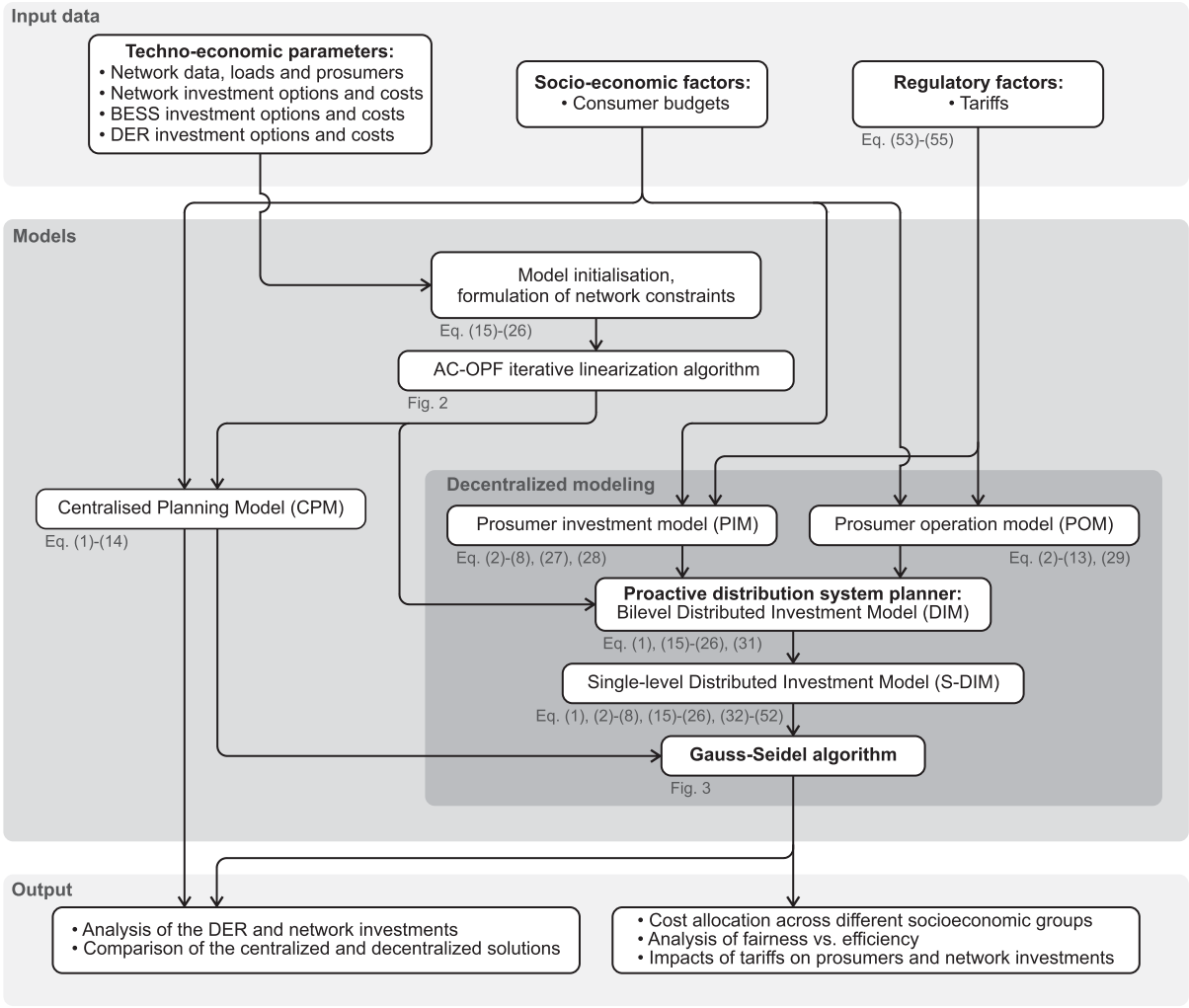

Fig. 1. Modeling framework overview.

MODEL: Centralized Planning Model (CPM) [LP].

Objective function

$$\min \sum_{l\in\mathcal{L}} A_l s_l + \sum_{n\in\mathcal{N}} A_n^R c_n + \sum_{i\in\mathcal{I}} (A_i^s p_i^s + A_i^B p_i^B) + \sum_{t\in\mathcal{T}} C_t^A (p_t^w - p_t^{in})\Delta_t + \sum_{t\in\mathcal{T}} C_t^R (r_t^w - q_t^{out})\Delta_t \quad (1)$$

Power balance

$$D_{i,t}^A = e_{i,t}^w + e_{i,t}^s - e_{i,t}^{in} - e_{i,t}^{ch} + e_{i,t}^{ds} \quad : \lambda_{i,t}^A \quad \forall i \in \mathcal{I}, t \in \mathcal{T} \quad (2)$$

$$D_{i,t}^R = r_{i,t}^w - r_{i,t}^{in} \quad : \lambda_{i,t}^R \quad \forall i \in \mathcal{I}, t \in \mathcal{T} \quad (3)$$

Budget

$$A_i^s p_i^s + A_i^B p_i^B \le K_i : \beta_i \quad \forall i \in \mathcal{I} \quad (4)$$

Solar PV

$$e_{i,t}^s \le p_i^s \psi_{i,t} \quad : \phi_{i,t}^s \quad \forall i \in \mathcal{I}, t \in \mathcal{T} \quad (5)$$

Non-negativeness

$$e_{i,t}^w, e_{i,t}^{in}, r_{i,t}^w, r_{i,t}^{in}, SoC_{i,t}$$

$$e_{i,t}^s, e_{i,t}^{ch}, e_{i,t}^{ds} \ge 0 \quad : \sigma_{i,t}^* \quad \forall i \in \mathcal{I}, t \in \mathcal{T} \quad (6)$$

$$p_i^s \ge 0 \quad : \sigma_i^s \quad \forall i \in \mathcal{I} \quad (7)$$

$$p_i^B \ge 0 \quad : \sigma_i^B \quad \forall i \in \mathcal{I} \quad (8)$$

CPM BESS operation

$$e_{i,t}^{ch} \le p_i^b \quad \forall i \in \mathcal{I}, t \in \mathcal{T} \quad (9)$$

$$e_{i,t}^{ds} \le p_i^b \quad \forall i \in \mathcal{I}, t \in \mathcal{T} \quad (10)$$

$$SoC_{i,t} \le H_i p_i^b \quad \forall i \in \mathcal{I}, t \in \mathcal{T} \quad (11)$$

$$SoC_{i,t+1} = SoC_{i,t} + \eta_i^B e_{i,t}^{ch} - e_{i,t}^{ds} \quad \forall i \in \mathcal{I}, t \in \mathcal{T} \setminus \{T\} \quad (12)$$

$$SoC_{i,1} = SoC_{i,T\Delta T} \qquad \forall i \in \mathcal{I} \tag{13}$$

Reactive compensator

$$c^{w}_{n,t}, c^{in}_{n,t} \leq c_n \qquad \forall n \in \mathcal{N}, t \in \mathcal{T} \tag{14}$$

Equation (5) limits PV generation, considering solar production availability $\psi_{i,t}$. Equations (6), (7), and (8) prevent some variables from taking negative values. Finally, note that the dual variables of (2)–(8) are used in this model, as will be discussed in greater detail in Section II-B2.

Additionally, (9)–(13) denote the operation of BESS in the CPM. Equations (9), (10), and (11) represent the upper limits for charging, discharging, and the state of charge of the BESS, respectively. The energy inventory of the BESS is represented by (12), and (13) imposes that the state of charge at the initial time and at the end of every day is the same. Finally, (14) represents the compensator limits.

The DN modeling incorporates a DistFlow approach proposed in [29], which introduces a convex non-linear formulation. To handle these non-linearities, the proposal presents an iterative algorithm for linearization studied in [30].

Consequently, the DN equations are represented with (15)–(26). Equations (15) and (16) depict the aggregated power injections of all users i connected to a bus n. Equation (17) establishes the upper and lower voltage limits. Current limits are defined in (18), whereas (19) and (20) address the nodal balance for active and reactive power, accounting for losses. Ohm's law for each node is represented in (21). Lastly, (22) and (23) depict the interconnection between the distribution and bulk power systems. (24) to (26) present the linearized version of the equations proposed in [30]. Specifically, (24) and (25) denote the feasible operational region of every line (conceptualized as a circumference with a radius of s_l within the P-Q plane), a concept explored in detail in [31].

Network constraints

$$d^{A}_{n,t} = \sum_{i \in \mathcal{I}} (e^{w}_{i,t} - e^{in}_{i,t}) N_{i,n} \qquad \forall n \in \mathcal{N}, t \in \mathcal{T} \tag{15}$$

$$d^{R}_{n,t} + c^{w}_{n,t} - c^{in}_{n,t} = \sum_{i \in \mathcal{I}} (r^{w}_{i,t} - r^{in}_{i,t}) N_{i,n} \qquad \forall n \in \mathcal{N}, t \in \mathcal{T} \tag{16}$$

$$\underline{v_n} \leq v_{n,t} \leq \overline{v_n} \qquad \forall n \in \mathcal{N}, t \in \mathcal{T} \tag{17}$$

$$i_{l,t} \leq \overline{i_l} \qquad \forall l \in \mathcal{L}, t \in \mathcal{T} \tag{18}$$

$$\sum_{l \in \mathcal{L}} p_{l,t} O_{n,l} + d^{A}_{n,t} = \sum_{l \in \mathcal{L}} (p_{l,t} - R_l i_{l,t}) I_{n,l} \qquad \forall n \in \mathcal{N}, t \in \mathcal{T} \tag{19}$$

$$\sum_{l \in \mathcal{L}} q_{l,t} O_{n,l} + d^{R}_{n,t} = \sum_{l \in \mathcal{L}} (q_{l,t} - X_l i_{l,t}) I_{n,l} \qquad \forall n \in \mathcal{N}, t \in \mathcal{T} \tag{20}$$

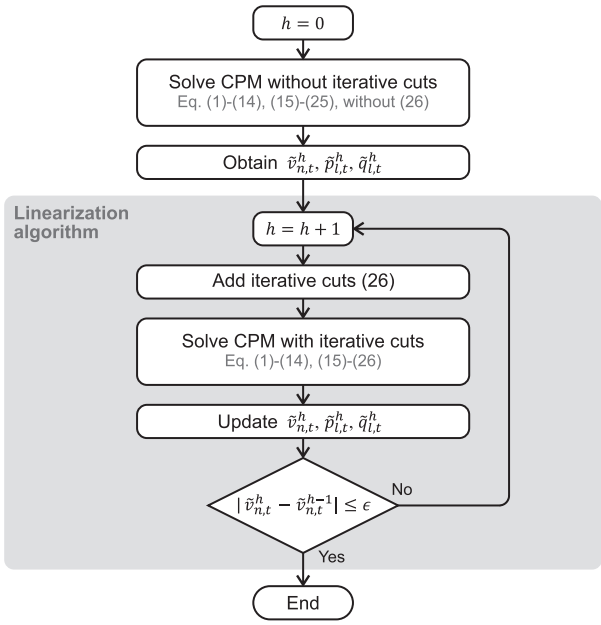

Fig. 2. Scheme of LP AC-OPF iterative algorithm.

$$\sum_{n \in \mathcal{N}} v_{n,t}(O_{n,l} - I_{n,l}) = 2R_l p_{l,t} + 2X_l q_{l,t} - (R_l^2 + X_l^2) i_{l,t} \qquad \forall l \in \mathcal{L}, t \in \mathcal{T} \tag{21}$$

$$\sum_{l \in \mathcal{L}} p_{l,t} O_{0,l} = p^{w}_{t} - p^{in}_{t} \qquad \forall t \in \mathcal{T} \tag{22}$$

$$\sum_{l \in \mathcal{L}} q_{l,t} O_{0,l} = q^{w}_{t} - q^{in}_{t} \qquad \forall t \in \mathcal{T} \tag{23}$$

$$q_{l,t} \leq \frac{-\alpha_k p_{l,t} + s_l}{\sqrt{1 - a_k^2}} \qquad \forall l \in \mathcal{L}, t \in \mathcal{T}, k \in \mathcal{A} \tag{24}$$

$$-\frac{-\alpha_k p_{l,t} + s_l}{\sqrt{1 - a_k^2}} \leq q_{l,t} \qquad \forall l \in \mathcal{L}, t \in \mathcal{T}, k \in \mathcal{A} \tag{25}$$

Iterative cuts

$$\Big(\sum_{n \in \mathcal{N}} \tilde{v}^h_{n,t} O_{n,l}\Big) i_{l,t} \geq (\tilde{p}^h_{l,t})^2 + 2\tilde{p}^h_{l,t}(p_{l,t} - \tilde{p}^h_{l,t}) + (\tilde{q}^h_{l,t})^2 + 2\tilde{q}^h_{l,t}(q_{l,t} - \tilde{q}^h_{l,t}) \qquad \forall l \in \mathcal{L}, t \in \mathcal{T} \tag{26}$$

Equation (26) imposes restrictions on apparent power through a line. The left-hand side encapsulates apparent power in relation to voltage $v_{n,t}$ and current $i_{l,t}$. Meanwhile, the right-hand side represents the operational boundary $p^2_{l,t} + q^2_{l,t}$ in the P-Q plane. These terms are linearized using an iterative approach explored in [30].

Fig. 2 presents a high level algorithm of the iterative process used to solve the AC-OPF problem. The iterative process begins with results obtained without considering constraint (26). Since

MODEL: Prosumer investment model (PIM). [NLP].

Objective function for prosumer i

$$\min A_i^s p_i^s + A_i^B p_i^B + \sum_{t\in\mathcal{T}}(\tau_{i,t}^D + \tau_{i,t}^E)e_{i,t}^w \Delta t - \sum_{t\in\mathcal{T}}(\tau_{i,t}^D + \varphi\tau_{i,t}^E)e_{i,t}^{in}\Delta t + \sum_{t\in\mathcal{T}}\tau_{i,t}^R(r_{i,t}^w - r_{i,t}^{in})\Delta t \quad (27)$$

Constraints: (2)–(8)

Prosumer BESS Operation

$$e_{i,t}^{ch} - e_{i,t}^{ds} = p_i^B \psi_{i,t}^B : \phi_{i,t}^B \qquad \forall i \in \mathcal{I}, t \in \mathcal{T} \quad (28)$$

MODEL: Prosumer operation model (POM).

Objective function for prosumer i

$$\min \sum_{t\in\mathcal{T}}(\tau_{i,t}^D + \tau_{i,t}^E)e_{i,t}^w \Delta t - \sum_{t\in\mathcal{T}}(\tau_{i,t}^D + \varphi\tau_{i,t}^E)e_{i,t}^{in}\Delta t + \sum_{t\in\mathcal{T}}\tau_{i,t}^R(r_{i,t}^w - r_{i,t}^{in})\Delta t \quad (29)$$

Constraints: (2)–(13)

this constraint serves as a lower limit for current, neglecting it implies that the variable is 0. Therefore, according to (21), this result indicates a lossless power flow. After this initialization, the algorithm proceeds to add cuts given by (26) on each iteration h. Note that cuts are given by the results of the CPM given by $\widetilde{p}_{l,t}$, $\widetilde{p}_{l,t}$, $\widetilde{v}_{n,t}$. Convergence is achieved with an accuracy determined by the tolerance ϵ for the voltage variation between successive iterations.

B. Decentralized Investment Model (DIM)

The DIM is formulated as a bilevel problem, which corresponds to a Stackelberg game between a proactive distribution planner (leader) and the prosumers (followers). The objective of the model is to identify an economic equilibrium between DER and DN investments. This section will describe the different components of the DIM, namely the lower level model, the upper level model, and reformulation of both models within a single level problem by means of Mathematical Programming with Equilibrium Constraints (MPEC).

1) Lower Level (prosumer) Model: This model represents the lower level, wherein there is one optimization model per prosumer i, and their outcomes include the investments p_i^s and p_i^B, as well as the operational variables $e_{i,t}^w$, $e_{i,t}^{in}$, $e_{i,t}^{ch}$, $e_{i,t}^{ds}$, $r_{i,t}^w$, and $r_{i,t}^{in}$.

Each prosumer is characterized by their demand patterns $D_{i,t}^A$ and $D_{i,t}^R$, their location in the network given by $N_{i,n}$, and their budget to invest in DER devices K_i. These features are often correlated with socioeconomic factors. For instance, different demand patterns $D_{i,t}^A$ and $D_{i,t}^R$ are associated with varying socioeconomic conditions [32], [33]. Similarly, the quality of a given distribution network is influenced by the socioeconomic characteristics of the households [34]. In this article, the focus is on the impact of the budget K_i, nevertheless, future work can analyze additional socioeconomic features mapped into the mentioned features.

The tariff schemes are represented with three arrays: $\tau_{i,t}^E$, $\tau_{i,t}^D$, and $\tau_{i,t}^R$, denoting the energy, distribution, and reactive power tariffs, respectively. Their detailed definitions depend on the specific regulatory framework being modeled.

The objective function is defined by (27), which incorporates DER investment, the energy bill calculated based on energy and DN tariffs, and revenue from energy exports. This revenue is valued at the energy tariff reduced by a factor φ.

Finally, the objective function includes the reactive energy balance.

It is noteworthy that tariffs vary for every user and time, thus they can be adjusted to a specific tariff definition. In addition, distribution tariff $\tau_{i,t}^D$ definitions are non-linear functions (usually defined in several regimes that originate non-linearities). Moreover, when equilibrium is reached, $\tau_{i,t}^D$ becomes a function of all prosumers' decisions, capturing economic relations among agents. Consequently, the prosumer model is a Non-Linear Programming (NLP) model.

Finally, the BESS operation is determined in (28) according to a power profile given by $\psi_{i,t}^B$, which is a time series with values in the interval [-1, 1] representing normalized charging and discharging rates. From the POM perspective, this profile is defined exogenously. This methodology, unlike eqs. (9)–(13), reduces the number of variables (no need to use $SoC_{i,t}$) and equations (replacing five inter-temporal constraints with a single intra-temporal constraint), thereby reducing the computational complexity.

In this regard, this article updates the profile $\psi_{i,t}^B$, optimizing the profile through a Prosumer Operation Model (POM). Note that the POM model considers a fixed amount of DER (p_i^S and p_i^B), and the BESS modeling utilizes the same equations used by CPM in (9)–(13). Thus, the battery profile $\psi_{i,t}^B$ is the normalized charging and discharging rates given by (30).

$$\psi_{i,t}^B = \frac{e_{i,t}^{ch} - e_{i,t}^{ds}}{p_i^B} \qquad \forall i \in \mathcal{I}, t \in \mathcal{T} \quad (30)$$

2) Upper Level (Proactive Distribution Planner) Model: The model considers a proactive distribution planner with a social perspective, meaning that it minimizes both network and prosumers cost. For this approach the planner considers as objective function the equation (1), with the key difference that optimal prosumer decisions from PIM are taken into account. Note that in other contexts, where a DSO minimizes only the network cost but keeping the prosumers decision decentralized, a similar approach can be found in [14]. Accordingly, the DIM is a bilevel NLP due to (31) (considering optimal prosumers' decisions).

It is noteworthy that, in this paper, the distribution network does not include the installation of BESS as part of its portfolio. While current regulations, particularly within the EU, may permit grid operators to own BESS for specific grid-support functions, they are generally prohibited from participating in energy markets with these assets to avoid conflicts of interest and ensure fair competition [35]. Future regulatory and infrastructure planning should account for these limitations and consider frameworks that enable the integration of BESS into the distribution network in a manner that supports grid reliability without compromising market integrity.

Unlike the CPM, the DIM represents the case where prosumers aim to minimize their energy bills without considering, or having knowledge of, the decisions of their peers.

MODEL: Bilevel Distributed Investment Model (DIM) [NLP].

Objective: (1)
Constraints: Network constraints: (15)–(26)

$$p_i^s, p_i^B, e_{i,t}^w, e_{i,t}^s, e_{i,t}^{in}, e_{i,t}^{ch}, e_{i,t}^{ds}, r_{i,t}^w, r_{i,t}^{in} \in \arg\min(\text{PIM}) \quad (31)$$

C. Solving DIM: Gauss-Seidel Algorithm

The bilevel DIM structure must be reformulated into a single-level problem to be solvable by commercial solvers [36]. However, this process is complicated by the distribution tariff, whose value depends on the prosumer's decisions making the problem non-linear. In fact, even in simple cases (for instance a tariff with linear dependence), the variable distribution tariff may introduce non-linearities to the problem formulation as the tariffs are multiplied by the net energy consumption which is also variable (27). Consequently, the single-level formulation becomes a mixed-integer nonlinear programming (MINLP) problem, which may lead to multiple Stackelberg equilibria.

To address this challenge, the article proposes an iterative Gauss-Seidel algorithm that solves the MINLP problem by breaking it into multiple mixed-integer linear programming (MILP) problem that can be solved iteratively whereas managing the non-linear components. The principles of this algorithm are similar to those in [37], which was applied in the context of generation market equilibrium under different carbon tax definitions. Likewise, authors in [38] explored the Gauss-Seidel algorithm for generalized Nash equilibrium problem.

For this purpose, it is initially assumed that $\tau_{i,t}^D$ is constant, which renders the POM linear and allows it to be replaced with the MPEC equations, which are given by the first-order conditions ((32) to (40)), and the linearized complementary slackness associated with (2)–(8) and (28) according to the Fortuny-Amat & McCarl linearization [39] using the big M technique ((41)–(52)). Thus, the resulting model becomes a single-level MILP.

Fig. 3 presents a schematic representation of the algorithm used to find the economic equilibrium, where boxes represent

MODEL: Single-level DIM (S-DIM) [MILP].

Objective function: (1)
Constraints: (2)–(8)
Network constraints: (15)–(26)
First order conditions

$$A_i^s + A_i^s \beta_i - \sum_{t\in\mathcal{T}} \psi_{i,t}^s \phi_{i,t}^s - \sigma_i^s = 0 \qquad \forall i \in \mathcal{I} \quad (32)$$

$$A_i^B + A_i^B \beta_i - \sum_{t\in\mathcal{T}} \psi_{i,t}^B \phi_{i,t}^B - \sigma_i^B = 0 \qquad \forall i \in \mathcal{I} \quad (33)$$

$$\tau_{i,t}^E + \tau_{i,t}^D - \lambda_{i,t}^A - \sigma_{i,t}^{e^w} = 0 \qquad \forall i \in \mathcal{I}, t \in \mathcal{T} \quad (34)$$

$$-\varphi\tau_{i,t}^E - \tau_{i,t}^D + \lambda_{i,t}^A - \sigma_{i,t}^{e^{in}} = 0 \qquad \forall i \in \mathcal{I}, t \in \mathcal{T} \quad (35)$$

$$\phi_{i,t}^s - \lambda_{i,t}^A - \sigma_{i,t}^{e^s} = 0 \qquad \forall i \in \mathcal{I}, t \in \mathcal{T} \quad (36)$$

$$\phi_{i,t}^B - \lambda_{i,t}^A - \sigma_{i,t}^{e^{ds}} = 0 \qquad \forall i \in \mathcal{I}, t \in \mathcal{T} \quad (37)$$

$$-\phi_{i,t}^B + \lambda_{i,t}^A - \sigma_{i,t}^{e^{ch}} = 0 \qquad \forall i \in \mathcal{I}, t \in \mathcal{T} \quad (38)$$

$$\tau_{i,t}^R - \lambda_{i,t}^R - \sigma_{i,t}^{r^w} = 0 \qquad \forall i \in \mathcal{I}, t \in \mathcal{T} \quad (39)$$

$$-\tau_{i,t}^R + \lambda_{i,t}^R - \sigma_{i,t}^{r^{in}} = 0 \qquad \forall i \in \mathcal{I}, t \in \mathcal{T} \quad (40)$$

Linearized complementary slackness

$$A_i^s p_i^s + A_i^B p_i^B - K_i \geq M u_i^\beta \qquad \forall i \in \mathcal{I} \quad (41)$$

$$\beta_i \leq M(1 - u_i^\beta) \qquad \forall i \in \mathcal{I} \quad (42)$$

$$e_{i,t}^s - p_i^s \psi_{i,t}^s \geq M u_{i,t}^{\phi^s} \qquad \forall i \in \mathcal{I}, t \in \mathcal{T} \quad (43)$$

$$\phi_{i,t}^s \leq M(1 - u_{i,t}^{\phi^s}) \qquad \forall i \in \mathcal{I}, t \in \mathcal{T} \quad (44)$$

$$e_{i,t}^w, e_{i,t}^{in}, r_{i,t}^w, r_{i,t}^{in}, e_{i,t}^s, e_{i,t}^{ch}, e_{i,t}^{ds} \leq M u_{i,t}^{\sigma^*} \qquad \forall i \in \mathcal{I}, t \in \mathcal{T} \quad (45)$$

$$\sigma_{i,t}^* \leq M(1 - u_{i,t}^{\sigma^*}) \qquad \forall i \in \mathcal{I}, t \in \mathcal{T} \quad (46)$$

$$p_i^s \leq M u_i^{\sigma^s} \qquad \forall i \in \mathcal{I} \quad (47)$$

$$\sigma_i^s \leq M(1 - u_i^{\sigma^s}) \qquad \forall i \in \mathcal{I} \quad (48)$$

$$p_i^B \leq M u_i^{\sigma^B} \qquad \forall i \in \mathcal{I} \quad (49)$$

$$\sigma_i^B \leq M(1 - u_i^{\sigma^B}) \qquad \forall i \in \mathcal{I} \quad (50)$$

$$u_i^\beta, u_i^{\sigma^s}, u_i^{\sigma^B} \in \{0, 1\} \qquad \forall i \in \mathcal{I} \quad (51)$$

$$u_{i,t}^{\phi^s}, u_{i,t}^{\sigma^*} \in \{0, 1\} \qquad \forall i \in \mathcal{I}, t \in \mathcal{T} \quad (52)$$

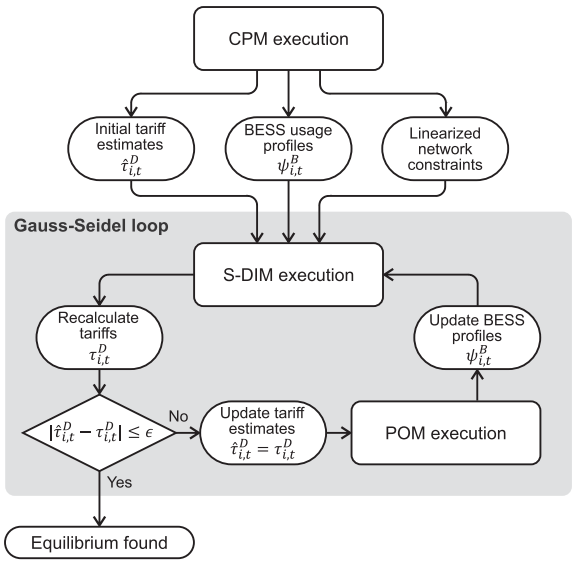

Fig. 3. Gauss-Seidel algorithm flowchart.

models and ovals represent parameters derived from model outputs. The process begins with a CPM execution, which serves as a benchmark of the Stackelberg equilibrium (see Fig. 1). This provides initial estimates for key parameters such as the distribution tariff $\hat{\tau}^D_{i,t}$ and BESS usage profile $\psi^B_{i,t}$. Note that those parameters may be initialized exogenously without the needs of CPM execution. These are then refined through an iterative Gauss-Seidel loop. If the recalculated distribution tariff $\tau^D_{i,t}$ converges (within a tolerance ϵ), the Stackelberg equilibrium is achieved. Otherwise, the algorithm continues with updated parameters via a POM execution. The full iterative flow is illustrated in the Fig. 3.

It is important to note that, in this context, the Gauss-Seidel algorithm serves as a practical approach to solve the original bilevel DIM problem—formulated as a nonlinear program (NLP)—through successive iterations of mixed-integer linear programs (MILPs), thereby reducing the original problem's complexity. While the algorithm does not provide a theoretical guarantee of convergence in non-convex settings, several factors can influence its practical convergence when applied to network and prosumer investment problems, as in this article. For instance, in small systems with limited prosumer diversity, the iterative algorithm may oscillate between two states, preventing convergence. In this regard, if the lower-level problem is convex [36], the equilibrium is unique; thus, in the event of convergence, the Gauss-Seidel algorithm will reach this unique equilibrium.

D. Tariffs Explored in This Work

Regarding the energy tariffs, this work explores three options. First, flat tariff during the whole year, corresponding to the average marginal cost of energy (MgC), weighted by the corresponding demand. Second, a 2-block tariff, or 2-b, which has two values across the day: a low value between midnight and 6:59 am, and a high value between 7:00 am and 11:59 pm. This scheme is based on the U.K.'s economy seven tariffs [40]. In both time windows, $\tau^E_{i,t}$ is equal to the average marginal cost. Finally, the third tariff is directly the MgC in every hour.

TABLE I
TARIFF EXPLORED IN THIS WORK

Distribution tariff	Vol 100 Peak 0			Vol 10 Peak 90		
Energy tariff	MgC	2-b	Flat	MgC	2-b	Flat

In this article, the reactive power tariff $\tau^R_{i,t}$ is assumed to be zero, which aligns with classical residential tariff structures. This simplification helps streamline the analysis while remaining consistent with practical tariff designs.

$$Vol_{i,t} = \frac{DN}{\sum_{t'} p^w_{t'} - p^{in}_{t'}} \tag{53}$$

$$Peak_{i,t} = \begin{cases} 0 & \text{if } p^w_t - p^{in}_t \leq P \\ \frac{DN}{\sum_{t' \in \mathcal{T}^P} p^w_{t'} - p^{in}_{t'}} & \text{otherwise} \end{cases} \tag{54}$$

$$\tau^D_{i,t} = \delta Vol_{i,t} + (1-\delta) Peak_{i,t} \tag{55}$$

Regarding the DN tariff, $\tau^D_{i,t}$ captures the network costs associated with meeting different demand levels. In this work, the combination of two mechanisms is explored. First, the volumetric tariff divides the cost of the DN by the total net electricity demand for the system as in (53). Second, the peak tariff divides the cost of the DN by the sum of the net electricity demand over a threshold P (i.e., when $p^w_t - p^{in}_t \geq P$, see 54). Therefore, during those times when net demand is lower than a threshold P, the peak demand is 0. In this article, the threshold is defined as the 90th percentile of net electricity demand during the peak day, which corresponds to the three highest demand hours on that day. This assumption aligns with practical applications, such as the five coincident peaks used by the system operator in Pennsylvania, New Jersey, and Maryland (PJM) [41], and the electricity triads applied by National Energy System Operator (NESO) in Great Britain [42]. In both cases, a set of peak hours is considered rather than a single value.

Thus, two linear combinations for the distribution tariff are explored as stated in 55, with δ equal to 100% (namely Vol 100 Peak 0) and 10% (Vol 10 Peak90).

Finally, Table I shows the six different tariffs explored in this work, considering three tariffs for energy and two for distribution. Note that whereas the algorithm is capable of handling tariffs with different prices for each prosumer, for the sake of simplicity and to make the results more intuitive, in this article, the tariffs are assumed to be uniform across all users. However, future analyses could incorporate more sophisticated tariff structures. For instance, distribution tariffs may reflect zonal cost differences [43], [44], or include reductions for vulnerable groups to promote equity [45]. In such cases, the distribution tariff $\tau^D_{i,t}$ for prosumer i would depend on the specific tariff definition, resulting in user-specific values. Nevertheless, the proposed model remains applicable under these more complex tariff scenarios.

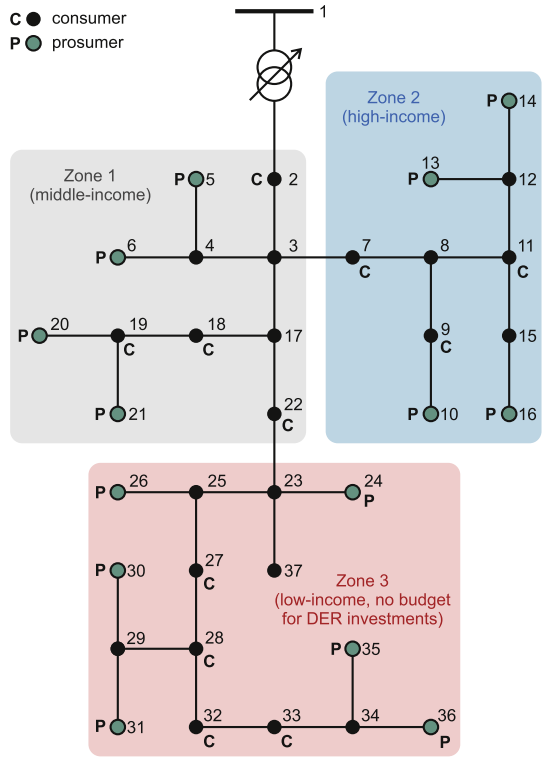

Fig. 4. IEEE 37-bus feeder scheme.

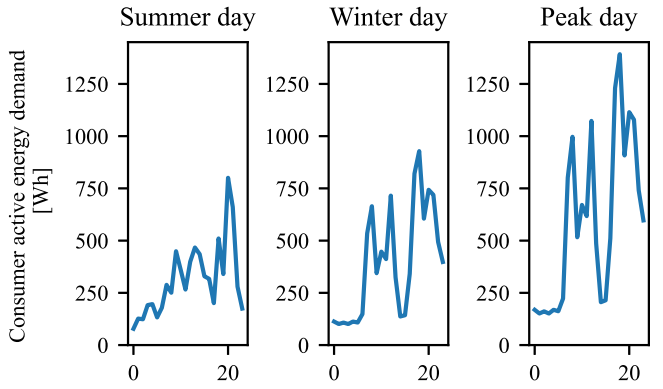

Fig. 5. Demand for every prosumer and consumer of the three representative days. The x-axis represents 24 hours.

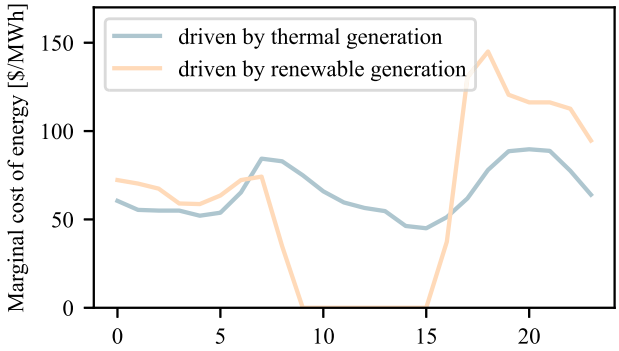

Fig. 6. Marginal costs scenarios. The x-axis represents 24 hours.

III. Results

A. Case Studies Definition

The studies presented in this work are conducted using a modified version of the IEEE 37-bus feeder [46], which includes 14 prosumers and 11 consumers. Four user classes are defined: no-budget (consumers), low-budget, middle-budget, and high-budget users. Three zones are arbitrarily defined to separate different neighborhoods where users have similar budgets (i.e., low, mid, and high). It is worth noting that consumers (no-budget users) are located in every neighborhood. Fig. 4 illustrates the network topology and the users' locations.

The energy needs of every user are represented by their active and reactive power demand ($D^A_{i,t}$ and $D^R_{i,t}$ with a power factor of 0.95 for every prosumer and consumer) for three representative days, obtained using the CREST demand model [47], which is a bottom-up model for simulating electricity demand in residential dwellings. These days correspond to typical summer and winter profiles, and peak demand conditions (see Fig. 5).

Energy can be procured from the bulk power system through the primary substation at the hourly marginal cost of energy C^A_t. Two different marginal cost sensitivities are studied, as shown in Fig. 6 The first sensitivity involves marginal costs varying between 50 and 85 $/MWh, which are typical cost ranges for thermal-based systems. The second sensitivity considers a marginal cost series equal to 0 $/MWh during the middle of the day (i.e., period with high solar generation outputs), rising to 150 $/MWh in the evening to keep the average marginal cost of the whole day. This case is inspired in a system with excess of renewable generation (solar PV). In both cases, the marginal cost has an average value of 65 $/MWh. Users purchase energy at the energy tariff $\tau^E_{i,t}$ and sell energy at a fraction $\varphi = 0.1$ of the energy tariff $\tau^E_{i,t}$. Reactive power marginal costs C^R_t are assumed to be 5% of the marginal cost of energy. $\tau^R_{i,t}$ is set to zero.

TABLE II
Location of Network Users and Their Budget Per Zone

User	Annuitized budget	Tag
Consumers	$0	No budget
Prosumers zone 1	$50	Middle-budget
Prosumers zone 2	$100	High-budget
Prosumers zone 3	$25	Low-budget

Additionally, the DN investment costs are set to $A_l = 90$ $/kW-km-yr. For the $l = 0$, A_l accounts for the transformer cost. Additional information and technical parameters can be found in the case study repository [48]. It is worth mentioning that given the long-term view, the network is planned from scratch in a greenfield fashion. This approach is utilized in Chile and other Latin American countries [49].

The budget K_i per user is provided in Table II. The PV investment costs A^s_i are set to 150 $/kW-yr according to current conditions [50]. The BESS costs are set as A^B_i at 120 $/kW-yr, and the capacity H_i is 4 hours.

B. Analyses Performed

Tariff structures and non-cooperative strategies influence *system-level* costs. However, these costs may not be evenly distributed among users. At the *user-level*, some users may benefit (comparing their costs with no DER installation), while others bear higher costs due to inefficiencies (sub-optimal solutions) and the benefits enjoyed by other users. This section quantifies these effects through two analyses:

1) System-Level Analyses: This section demonstrates *Stackelberg inefficiencies*, defined as the difference between the total costs of the CPM and DIM. Stackelberg inefficiencies are quantified for six combinations of energy and distribution tariffs, considering solar PV and BESS as DER technologies. The equilibrium is compared against two benchmarks:

a) The scenario where no user invests in DER (No DER installations).
b) The scenario where DER investment results from the CPM (CPM costs).

2) User-Level Analyses: This section explores the distribution of costs among users with different budgets (no, low-, mid-, and high-budget). Total billing costs and DN cost allocation for the six different tariffs are compared. Additionally, as a benchmark, the scenario where there is no DER investment (all users are charged the same amount) is considered. This allows us to analyze if DER has improved the economic position of specific users. Meanwhile, CPM is not considered as a benchmark, as this is not an equilibrium.

3) Sensitivity of Marginal Cost of Energy: This section explores the robustness of the conclusions by analyzing the equilibrium when marginal energy costs are driven by renewable generation (see Fig. 6). In this context, the main trends in efficiency and equity are compared with the base case, where marginal costs are driven by thermal generation.

4) Computational Performance: This section examines the computational performance of the algorithm, highlighting key variables affecting computational burden and presenting exploratory results of the proposal.

C. System-Level Analyses

Fig. 7 shows the system-level costs. The CPM cost is 10.2 k$-yr (red dashed line), representing savings of 4.5% compared to the no DER costs (green dashed line). Meanwhile, DIM costs are approximately 1.9% higher than the CPM cost. These results highlight the importance of a holistic review of tariffs and the undesirable effects of updating only one component of the tariff. For instance, with the distribution tariff Vol 100 Peak 0 (Fig. 7, left), total system costs remain the same regardless of the energy tariff. Conversely, for Vol 10 Peak 90 (Fig. 7, right), total system costs for the 2-b and flat energy tariffs are higher compared to the volumetric tariff. Thus, partial modifications of tariffs could lead to a more inefficient equilibrium, even if the change is "in the right direction".

DER investment (Fig. 8) strongly depends on the tariff arrangement. When the distribution tariff is Vol 100 Peak 0, Fig. 8 shows a massive deployment of solar PV without storage installation, regardless of the energy tariff.

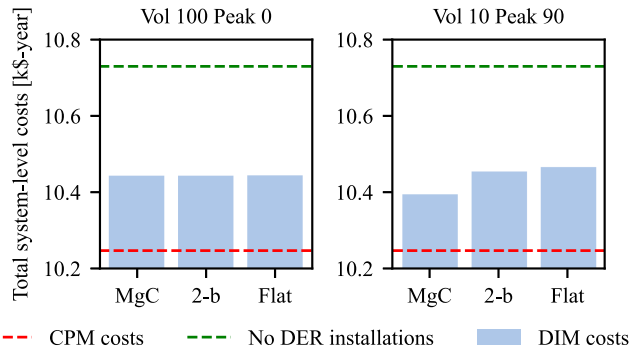

Fig. 7. The figure illustrates the total system-level costs. The distribution tariff is specified at the top of each chart. The x-axis represents the energy tariff. The red dashed line indicates the CPM cost, while the green dashed line represents the system-level cost in the absence of DER investments.

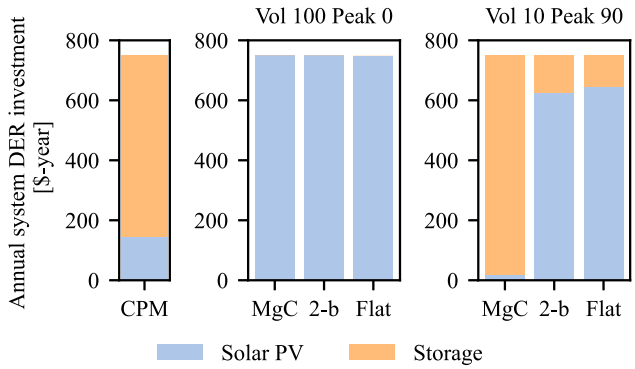

Fig. 8. The figure illustrates investment in DER in stacked bars. The analyzed cases are the CPM investments (left), the equilibrium investment for the Vol 100 Peak 0 distribution tariff (middle), and the Vol 10 Peak 90 distribution tariff (right).

The explanation lies in the comparison between the total tariff paid by prosumers and the Levelized Cost of Energy (LCOE) of solar PV technology. Fig. 9 presents various tariff structures throughout a typical day and during the peak day. It is important to note that, in this study, tariffs are uniform across all prosumers, as indicated by equations (53), (54), (55) . Additionally, in each case, the LCOE associated with solar PV is also shown.

In the scenario with a distribution tariff of Vol 100 Peak 0, prosumers choose to deploy solar PV because its LCOE (42 $/MWh) is lower than both the import and export tariffs. This is illustrated in the first column of Fig. 9, where the LCOE—represented by the red dashed line—remains below the tariff levels at all times.

Conversely, for the Vol 10 Peak 90 distribution tariff, the solar PV LCOE is between the total export and import tariffs. In this case, prosumers are incentivized to install DER for self-consumption only. Thus, BESS installation depends on the energy tariff. With flat and 2-b energy tariffs, only a small fraction of the total budget is invested in storage, driven by the high peak of the distribution tariff during peak days. For flat or 2-b electricity tariffs, there are no incentives for energy arbitrage. Meanwhile, with the MgC energy tariff, incentives

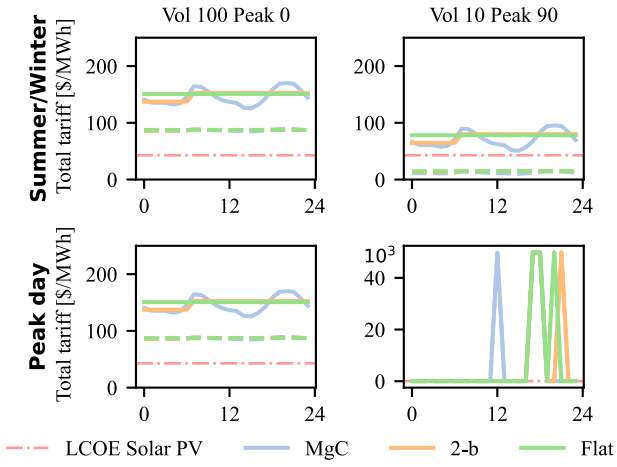

Fig. 9. The charts depict the obtained tariffs after solving the DIM model (Stackelberg's equilibrium). The first column shows the Vol 100 Peak 0 distribution tariff, and the second column shows the Vol 10 Peak 90 distribution tariff. The top row indicates the summer/winter period, and the bottom row shows the peak day. Each chart displays the LCOE of solar PV (red dashed line). For each energy tariff, the total tariff for imports is shown with a continuous line, and the export tariff with a dashed line. Exports are valued at $\varphi\tau^{E}_{i,t} + \tau^{D}_{i,t}$. The x-axis represents the 24 hours of a day.

for BESS investment increase because energy arbitrage can be included in the prosumer's revenue stream.

Finally, it is worth noting the higher peaks of Vol 10 Peak 90 during the peak day (see Fig. 9, bottom right chart). In this context, BESS systems receive the price signal to operate accordingly, thereby helping the system defer DN investments.

Remarkably, in all the above-mentioned cases, the network did not require reactive compensators to meet statutory voltage limits, as the voltage remained within the feasible operating range. To be specific, in this case study, node 1 presented a voltage of 1.03 per unit, which is the node with the highest voltage. Given the low demand levels, the voltage at the extreme nodes (nodes 30 to 37) showed a maximum voltage drop of only 0.1% during the peak day.

D. User-Level Analysis

The results of this section highlight that, even if the impact on efficiency in terms of cost is limited, tariffs have a significant impact on cost allocation among users.

Fig. 10 shows the distribution of system costs for different DER budgets and tariff schemes. Note that even though the tariff values are uniform across prosumers, net energy demand varies across socioeconomic sectors, driven by differences in DER installation. As a result, the actual costs faced by prosumers differ depending on their socioeconomic group. Therefore, the figure presents the average cost, grouped by budget level. The same applies to Fig. 11, which shows the average distribution cost.

In Fig. 10, the charts illustrate that the distribution network tariff plays a key role in the equity of system cost allocation. The most unequal solution occurs when the distribution tariff is purely volumetric (Vol 100 Peak 0). In this case, there is a

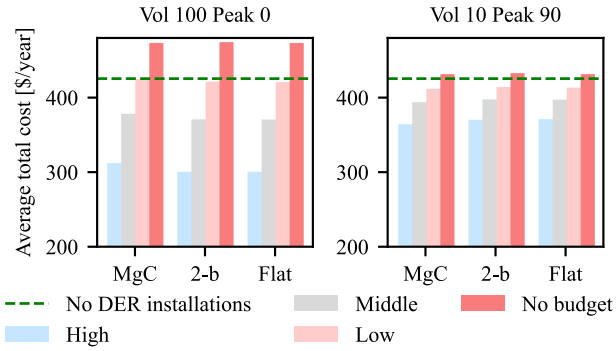

Fig. 10. The figure depicts the average total cost per user with different budgets to invest in DER. The distribution tariff is specified at the top of each chart, and the energy tariff is shown at the bottom. The red dashed line represents the cost when there is no DER deployment, and therefore, all users face the same cost.

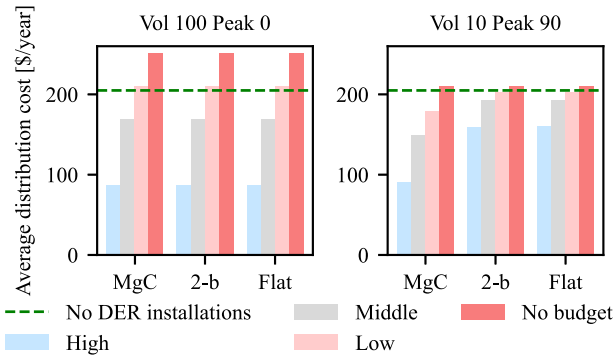

Fig. 11. The figure depicts the average distribution network cost per user with different budgets to invest in DER. The distribution tariff is specified at the top of each chart, and the energy tariff is shown at the bottom. The red dashed line represents the cost when there is no DER deployment, and therefore, all users face the same distribution cost.

cost gap between high- and no-budget users, where high-budget users face costs 35% lower than no-budget users.

This cost gap between high- and no-budget users is reduced when Vol 10 Peak 90 is applied. With the 2-b or flat energy tariffs, the gap is around 14%. For the MgC energy tariff, the gap reaches 16%. This difference is due to the extra revenue high-budget users earn through energy arbitrage with batteries.

Another aspect to consider is the additional costs paid by no-budget (and in some cases, low-budget) users compared to the no-DER installation scenario. For instance, no-budget users have to pay $46 more per year when the Vol 100 Peak 0 distribution tariff is applied (see Fig. 10, right), representing 10.9% more than the no-DER installation scenario. This extra cost comes directly from the additional cost of distribution charges. Fig. 11 shows the DN charges under different tariff schemes. For Vol 100 Peak 0 (Fig. 11, left), no-budget users pay $46 more per year in DN charges compared to the no-DER solution, demonstrating that the additional cost is due to network charges. A similar analysis for high-budget users shows that they save an average of $53 per year with the Vol 100 Peak 0 distribution tariff (Fig. 10, left), representing 29.5% less than the no-DER installation scenario. Of this, $35 per year are savings in distribution charges, while

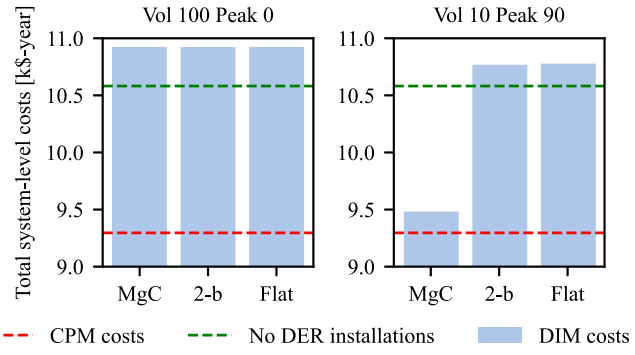

Fig. 12. The figure illustrates the system-level cost for the case of marginal cost driven by renewable generation. The distribution tariff is specified at the top of each tariff. The x-axis represents the energy tariff. The red dashed line indicates the CPM cost, while the green dashed line represent the system-level cost in the absence of DER investment.

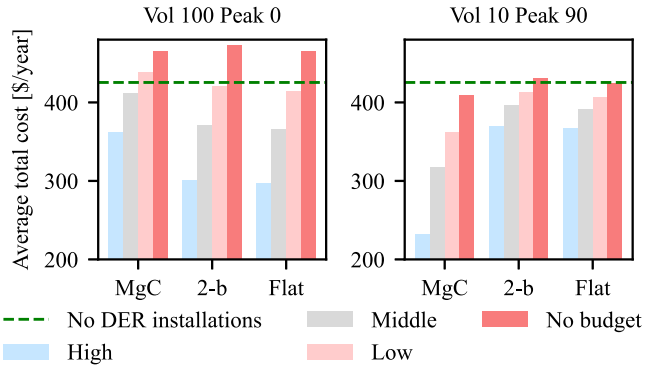

Fig. 13. The figure depicts the average total cost per user with different budgets to invest in DER for the case when the marginal costs are driven by renewable generation. The distribution tariff is specified at the top of each chart, and the energy tariff is shown at the bottom. The red dashed line represents the cost when there is no DER deployment, and therefore, all users face the same cost.

the remaining $18 per year are related to benefits from the energy tariff component.

Conversely, when Vol 10 Peak 90 is applied, there are minor additional costs for no-budget users (around $5 per year, about 1% of no-DER costs), fully explained by distribution charges (Fig. 11, right). For other users, their savings are explained by a mix of energy and distribution network charges.

These results underscore the importance of cost-reflective tariffs in reducing cross-subsidies in the undesired direction—that is, from no-budget users to high-budget users. These cross-subsidies arise from the way network costs are allocated among all prosumers and consumers. Distorted tariffs, such as the Vol 100 Peak 0 structure, lead to a cross-subsidy in network charges, with no-budget users effectively subsidizing high-budget users.

E. Sensitivity of Marginal Cost of Energy

To analyze the robustness of the conclusions presented above, a sensitivity analysis of the results to the considered marginal energy costs is performed. The system-level costs results are shown in Fig. 12. These results reinforce the importance of a holistic approach to tariff design.

For instance, taking as a reference the scheme based on a flat energy tariff combined with a Vol 100 Peak 0 distribution network tariff, a partial change involves modifying either the energy tariff or the distribution tariff, but not both. In this case, a partial change in the energy tariff has a negligible impact on system costs. Similarly, a partial adjustment of the distribution tariff to a Vol 10 Peak 90 configuration reduces costs by only 1.3%. In contrast, a holistic shift toward a cost-reflective tariff—using a MgC energy tariff combined with a Vol 10 Peak 90 distribution tariff—leads to a 13.1% reduction in system costs.

Focusing on this sensitivity analysis, a noteworthy finding is that certain tariff structures can lead to higher system costs than in scenarios where prosumers do not install distributed energy resources (DER). In such cases, the tariffs incentivize prosumers to install solar PV even when the marginal cost of energy during the day is zero, simply because the tariff remains higher than the LCOE of solar PV. As a result, the LCOE of energy injected by prosumers becomes more expensive than the energy available from the bulk power system.

It is important to note that when tariffs are cost-reflective, the incentives are aligned with system costs. Consequently, the resulting equilibrium is less expensive compared to any other studied tariff scheme.

The user-level analysis is shown in Fig. 13. It is observed that cost allocation across different socioeconomic groups changes with the tariff design, thereby affecting the distributional aspects of the resulting equilibrium. Using the Flat energy tariff and Vol 100 Peak 0 distribution tariff as the base case, high-budget prosumers pay, on average, 36% less than no-budget prosumers (referred to as the cost gap). When only the energy tariff is changed to the MgC energy tariff, the cost gap decreases to 22%. Alternatively, modifying only the distribution tariff to Vol 10 Peak 90 reduces the gap to 14%.

Interestingly, in the case of a fully cost-reflective tariff (MgC energy tariff combined with Vol 10 Peak 90), the attractiveness of the results depends on the perspective of fairness or equity. In this scenario, high-budget prosumers pay 44% less than no-budget prosumers, indicating a highly unequal outcome. However, it is important to note that even no-budget prosumers benefit from reduced average energy costs, despite being unable to invest in DER. This is due to reduced network costs, as other prosumers install batteries to avoid network reinforcements. Consequently, the fairness of the equilibrium depends on the chosen social objectives and how fairness is defined within the policy framework.

It is also worth noting that the user-level results highlight how cost-reflective tariffs reduce cross-subsidies from no-budget to high-budget prosumers, reinforcing the findings obtained under marginal costs driven by thermal generation. In fact, when the energy tariff is set to MgC and the distribution tariff to Vol 10 / Peak 90, no-budget prosumers see a reduction in their costs compared to the scenario in which no prosumers install DER. This suggests the emergence of cross-subsidies from high-budget to no-budget prosumers—an outcome that may fulfill a valuable social role.

TABLE III
EXECUTION TIME [S]

Distribution network tarfff	Vol 100 Peak 0			Vol 10 Peak 90		
Energy tariff	MgC	2-b	Flat	MgC	2-b	Flat
Execution time [s]	62	58	56	692	133	105

For solving the single level DSM with gauss-seidel algorithm.

F. Gauss-Seidel Algorithm Performance

The studies were performed on an Apple M1 Pro laptop with 16 GB RAM. Table III shows the time to converge for a single-level DIM using the proposed Gauss-Seidel algorithm. In general, the algorithm increases its complexity with the granularity of the tariffs. In this sense, the peak tariff implies higher computational times compared with purely volumetric cases. The energy tariff also impacts the computational burden, with the MgC energy tariff being the more complex (up to 5 times the computation times utilized by the 2-b energy tariff).

IV. DISCUSSION

In this article, the proposed DIM formulation corresponds to a deterministic model, where a proactive distribution network planner has perfect information, prosumers make rational decisions to minimize their costs, and their investments are limited by their budgets, which is the case in jurisdictions without specific mechanism such as feed-in-tariff or special subsidies to DER. In this context, the DIM solution represents a Stackelberg equilibrium, allowing for an assessment of the efficiency and fairness of the equilibrium under the stated assumptions.

Focusing on the case study, rather than on the modeling considerations, it analyzes DER deployment through a set of homogeneous prosumers, distinguished by their location and investment budgets for DER. This assumption is useful for examining how income differences influence DER adoption levels. However, the conclusions derived from the model should be interpreted having in mind homogeneous prosumers assumption and socioeconomic factors characterized by the budget only. Therefore, rather than focusing on numerical outcomes for specific individual, the presented results and analysis emphasize general trends in how the Stackelberg equilibrium is comparatively affected at both the system and user levels.

The proposed model allows us to draw two main conclusions that remain consistent across the sensitivity studies (i.e., variations in the marginal cost of energy). Firstly, it is essential to analyze tariffs as a whole—including both energy and distribution components—rather than treating them as isolated elements. It is also crucial to assess their impacts at both the system and user levels. Partial updates to either the energy or distribution component carry the risk of unintended outcomes, such as the integration of DERs without system-level benefits, which may also negatively impact vulnerable users.

Secondly, cost-reflective tariffs can potentially reduce cross-subsidies from low- to high-budget users. This is a significant result, considering that volumetric distribution tariffs and flat tariffs are distortive and still widely used (for instance, these are common in Latin America [49]). When such tariffs are in place, in the Stackelberg equilibrium, low-budget prosumers bear additional costs associated with DERs (related to network costs shared with other prosumers). A cost-reflective tariff improves this situation by reducing the burden placed on low-budget prosumers.

In this context, the role of the proposed model is to serve as a tool to support the tariff-setting process, providing a means to quantify the potential efficiency and fairness of a given tariff scheme and to create benchmarks for comparing different tariff options. Likewise, minor modifications to the objective function can be made to allow the proposed model to only capture the perspective of a distribution system owner (e.g., by removing the terms related to prosumer investments).

It is important to emphasize that this article the focus is on the impact of budget distribution across different consumers groups. However, other socioeconomic factors may also influence the equilibrium. Prosumers may be motivated to change their energy consumption patterns by various factors beyond their income. For instance, as explored in [32] some factors that may influence electricity demand patterns include economic capacity and energy costs, as well as climate and dwelling location, physical dwelling characteristics, household activities and services, and socio-demographic traits (e.g., education, age of inhabitants), among others. Consequently, further analysis is required to incorporate a set socioeconomic factors and to generate more comprehensive findings.

Likewise, Stackelberg models can be understood as a subset of broader models in which prosumers may pursue objectives beyond cost minimization. In this regard, agent-based models [51] offer a framework for incorporating behavioral aspects.

V. CONCLUSION

This paper investigates the long-term equilibrium of DER and DN capacity expansions, focusing on consumers with varying budget constraints for DER investments. To support this analysis, we propose a novel equilibrium model incorporating budget limitations while considering detailed AC power flow calculations over the DN. This is critical, as the DN's high R/X ratio prevents the use of linearized power flow models. Additionally, we propose a solution strategy employing a Gauss-Seidel algorithm to address certain non-linear terms within the model formulation. While this algorithm itself is well-established, its application in this context is innovative, enhancing its significance and contributing to the overall methodological framework.

Through multiple case studies, we observe significant impacts of tariff schemes and budget levels on long-term equilibrium outcomes. In this regard, the conclusions highlight the risk associated with tariff-setting process by quantifying the efficiency and cost allocation among prosumers of the long-term equilibrium. Likewise, through the analysis it is possible to observe how cost-reflective tariffs tends to diminish cross subsidies in unintended direction (from low to high-budget prosumers), diminishing the relative cost of low-budget prosumers.

Future studies could explore the inclusion of behavioral elements in assessing the long-term equilibrium of prosumer investments, as well as non-financial aspects, such as a more

detailed characterization of demand across different socioeconomic groups.

REFERENCES

[1] S. Burger, I. Schneider, A. Botterud, and I. Pérez-Arriaga, "Chapter 8 - fair, equitable, and efficient tariffs in the presence of distributed energy resources," in *Consumer, Prosumer, Prosumager*, F. Sioshansi, Ed. Academic Press, 2019, pp. 155–188, doi: 10.1016/B978-0-12-816835-6.00008-5.

[2] S. -E. Razavi et al., "Impact of distributed generation on protection and voltage regulation of distribution systems: A review," *Renew. Sustain. Energy Rev.*, vol. 105, pp. 157–167, 2019.

[3] R. Rana, I. B. Sperstad, B. N. Torsæter, and H. Taxt, "Economic assessment of integrating fast-charging stations and energy communities in grid planning," *SEGAN*, vol. 35, 2023, Art. no. 101083.

[4] O. Vågerö and M. Zeyringer, "Can we optimise for justice? Reviewing the inclusion of energy justice in energy system optimisation models," *Energy Res. Soc. Sci.*, vol. 95, 2023, Art. no. 102913.

[5] V. Azarova, D. Engel, C. Ferner, A. Kollmann, and J. Reichl, "Exploring the impact of network tariffs on household electricity expenditures using load profiles and socio-economic characteristics," *Nature Energy*, vol. 3, no. 4, pp. 317–325, 2018.

[6] M. Ansarin, Y. Ghiassi-Farrokhfal, W. Ketter, and J. Collins, "A review of equity in electricity tariffs in the renewable energy era," *Renew. Sustain. Energy Rev.*, vol. 161, 2022, Art. no. 112333.

[7] B. R. Alexander, "Dynamic pricing? Not so fast! A residential consumer perspective," *Electricity J.*, vol. 23, pp. 39–49, 2010.

[8] M. Ventosa, P. Linares, and I. J. Pérez-Arriaga, *Power System Econ.* London: Springer, 2013, pp. 47–123.

[9] R. Faia, F. Lezama, J. Soares, T. Pinto, and Z. Vale, "Local electricity markets: A review on benefits, barriers, current trends and future perspectives," *Renew. Sustain. Energy Rev.*, vol. 190, 2024, Art. no. 114006.

[10] J. Hönen, J. L. Hurink, B. Zwart, and B. Z. BertZwart, "A classification scheme for local energy trading," *OR Spectr.*, vol. 45, pp. 85–118, 2022.

[11] S. Cui, Y. -W. Wang, and N. Liu, "IET renewable power generation distributed game-based pricing strategy for energy sharing in microgrid with PV prosumers," *IET Renew. Power Gener*, vol. 12, pp. 380–388, 2017.

[12] N. Liu, M. Cheng, X. Yu, J. Zhong, and J. Lei, "Energy-sharing provider for PV prosumer clusters: A hybrid approach using stochastic programming and Stackelberg game," *IEEE Trans. Ind. Electron.*, vol. 65, no. 8, pp. 6740–6750, Aug. 2018.

[13] M. Askeland, S. Backe, S. Bjarghov, K. B. Lindberg, and M. Korpås, "Activating the potential of decentralized flexibility and energy resources to increase the EV hosting capacity: A case study of a multi-stakeholder local electricity system in Norway," *Smart Energy*, vol. 3, 2021, Art. no. 100034.

[14] M. Askeland, S. Backe, S. Bjarghov, and M. Korpås, "Helping end-users help each other: Coordinating development and operation of distributed resources through local power markets and grid tariffs," *Energy Econ.*, vol. 94, 2021, Art. no. 105065.

[15] P. Pediaditis, D. Papadaskalopoulos, A. Papavasiliou, and N. Hatziargyriou, "Bilevel optimization model for the design of distribution use-of-system tariffs," *IEEE Access*, vol. 9, pp. 132928–132939, 2021.

[16] S. Ramírez-López, G. Gutiérrez-Alcaraz, M. Gough, M. S. Javadi, G. J. Osório, and J. P. S. Catalão, "Bi-level approach for flexibility provision by prosumers in distribution networks," *IEEE Trans. Ind. Appl*, vol. 60, no. 2, pp. 2491–2500, Mar./Apr. 2024.

[17] J. Sepúlveda, L. Brotcorne, and H. Le Cadre, "A reverse Stackelberg model for demand response in local energy markets," *Eur. J. Oper. Res.*, vol. 327, no. 1, pp. 352–366, 2025, doi: 10.1016/j.ejor.2025.06.017. [Online]. Available: https://www.sciencedirect.com/science/article/pii/S0377221725004898

[18] T. Schittekatte, I. Momber, and L. Meeus, "Future-proof tariff design: Recovering sunk grid costs in a world where consumers are pushing back," *Energy Econ.*, vol. 70, pp. 484–498, 2018.

[19] T. Schittekatte and L. Meeus, "Least-cost distribution network tariff design in theory and practice," *Energy J.*, vol. 41, no. 5, pp. 119–156, 2020.

[20] H. L. Cadre, "On the efficiency of local electricity markets under decentralized and centralized designs: A multi-leader Stackelberg game analysis," *CEJOR*, vol. 27, pp. 953–984, 2019.

[21] M. Zugno, J. M. Morales, P. Pinson, and H. Madsen, "A bilevel model for electricity retailers' participation in a demand response market environment," *Energy Econ.*, vol. 36, pp. 182–197, 2013.

[22] D. Aussel, L. Brotcorne, S. Lepaul, and L. von Niederhäusern, "A trilevel model for best response in energy demand-side management," *Eur. J. Oper. Res.*, vol. 281, pp. 299–315, 2020.

[23] M. F. Anjos, L. Brotcorne, and J. A. Gomez-Herrera, "Optimal setting of time-and-level-of-use prices for an electricity supplier," *Energy*, vol. 225, 2021, Art. no. 120517.

[24] S. Doménech Martıńez, F. A. Campos, J. Villar, and M. Rivier, "Joint energy and capacity equilibrium model for centralized and behind-the-meter distributed generation," *Int. J. Elect. Power Energy Syst.*, vol. 131, 2021, Art. no. 107055.

[25] S. Doménech Martıńez, F. A. Campos, J. Villar, and M. Rivier, "An equilibrium approach for modeling centralized and behind-the-meter distributed generation expansion," *Electr. Power Syst. Res.*, vol. 184, 2020, Art. no. 106337.

[26] G. Strbac, C. V. Konstantinidis, R. Moreno, I. Konstantelos, and D. Papadaskalopoulos, "It's all about grids: The importance of transmission pricing and investment coordination in integrating renewables," *IEEE Power Energy Mag.*, vol. 13, no. 4, pp. 61–75, Jul./Aug. 2015.

[27] G. Elizondo and R. Poudineh, *Harnessing the Power of Distributed Energy Resources in Developing Countries: What can be Learned from the Experiences of Global Leaders.* Oxford, U.K.: Oxford Inst. Energy Studies, 2023.

[28] E. Sauma and S. Oren, "Proactive planning and valuation of transmission investments in restructured electricity markets," *J. Regulatory Econ.*, vol. 30, pp. 358–387, 2006.

[29] S. H. Low, "Convex Relaxation of Optimal Power Flow—Part II: Exactness," *IEEE Trans. Control Netw.*, vol. 1, no. 2, pp. 177–189, Jun. 2014.

[30] C. Carvallo, F. Jalil-Vega, and R. Moreno, "A multi-energy multi-microgrid system planning model for decarbonisation and decontamination of isolated systems," *Appl. Energy*, vol. 343, 2023, Art. no. 121143.

[31] R. Moreno, R. Moreira, and G. Strbac, "A MILP model for optimising multi-service portfolios of distributed energy storage," *Appl. Energy*, vol. 137, pp. 554–566, 2015.

[32] I. Khan, "Household factors and electrical peak demand: A review for further assessment," *Adv. Building Energy Res.*, vol. 15, no. 4, pp. 409–441, 2021.

[33] M. Sánchez-López et al., "The diverse impacts of COVID-19 on electricity demand: The case of Chile," *Int. J. Elect. Power Energy Syst.*, vol. 138, 2022, Art. no. 107883.

[34] A. M. Brockway, J. Conde, and D. Callaway, "Inequitable access to distributed energy resources due to grid infrastructure limits in California," *Nature Energy*, vol. 6, no. 9, pp. 892–903, 2021.

[35] European University Institute. Robert Schuman Centre for Advanced Studies., "The EU clean energy package," Publications Office, Lu, 2018, doi: 10.2870/013463.

[36] A. Ehrenmann, *Equilibrium Problems with Equilibrium Constraints and their Application to Electricity Markets.* Cambridge, U.K.: Univ. Cambridge, 2004.

[37] G. Diaz, F. D. Muñoz, and R. Moreno, "Equilibrium analysis of a tax on carbon emissions with pass-through restrictions and side-payment rules," *Energy J.*, vol. 41, no. 2, pp. 93–122. 2020.

[38] J. Nie, X. Tang, and L. Xu, "The Gauss–Seidel method for generalized Nash equilibrium problems of polynomials," *Comput. Optim. Appl.*, vol. 78, pp. 529–557, 2021.

[39] J. Fortuny-Amat and B. McCarl, "A representation and economic interpretation of a two-level programming problem," *J. Oper. Res. Soc.*, vol. 32, no. 9, pp. 783–792, 1981.

[40] "Economy 7 consumer guide ofgem," 2023. [Online]. Available: https://bit.ly/3rzeKg0

[41] *PJM Operator System, PJM Manual 18: PJM Capacity Market.* Valley Forge, PA, USA: PJM Interconnection, L.L.C., 2022.

[42] National Energy System Operator, "Public what are electricity triads," London, U.K., Feb. 2025.

[43] V. S. Etchebehere and J. W. M. Lima, "Locational tariff structure for radial network fixed costs in a DER context," *IEEE Access*, vol. 10, pp. 597–607, 2022.

[44] P. M. Sotkiewicz and J. M. Vignolo, "Towards a cost causation-based tariff for distribution networks with DG," *IEEE Trans. Power Syst.*, vol. 22, no. 3, pp. 1051–1060, Aug. 2007.

[45] C. Alvial-Palavicino and S. Ureta, "Economizing justice: Turning equity claims into lower energy tariffs in Chile," *Energy Policy*, vol. 105, pp. 642–647, 2017.

[46] K. P. Schneider et al., "Analytic considerations and design basis for the IEEE distribution test feeders," *IEEE Trans. Power Syst.*, vol. 33, no. 3, pp. 3181–3188, May 2018.
[47] E. McKenna, M. Thomson, and J. Barton, *CREST Demand Model*. Leicestershire, U.K.: Loughborough University, 2015. [Online]. Available: https://repository.lboro.ac.UK/articles/dataset/CREST_Demand_Model_v2_0/2001129
[48] M. Sanchez, *Tariff and Socioeconomic Factors: Tariff and Socioeconomic Factors in Equilibrium Anal. of DER Investments*. Manchester, U.K.: Univ. Manchester, 2025. [Online]. Available: https://github.com/miguelsanlopUoM/Tariff_and_SocioEconomic_Factors
[49] R. Moreno et al., "Distribution network rate making in Latin America: An evolving landscape," *IEEE Power Energy Mag.*, vol. 18, no. 3, pp. 33–48, May/Jun. 2020.
[50] A. Mey, *Average U. S. Construction Costs Drop for Solar, Rise for Wind and Natural Gas Generators.* Washington, DC, USA: U.S. Energy Inf. Admin., 2022. [Online]. Available: https://bit.ly/46oDfeM
[51] P. Ringler, D. Keles, and W. Fichtner, "Agent-based modelling and simulation of smart electricity grids and markets–A literature review," *Renewable Sustain. Energy Rev.*, vol. 57, pp. 205–215, 2016.

Miguel Sanchez-Lopez received the B.Sc. and M.Sc. degrees from Universidad de Chile, Santiago, Chile, and the Ph.D. degree from the University of Manchester, Manchester, U.K and Universidad de Chile. He is currently a Postdoctoral Research Associate with the University of Oxford, Oxford, U.K., where he focuses on the energy transition in low- and middle-income countries and regions affected by conflict.

Andrey Churkin (Member, IEEE) received the B.Sc. and M.Sc. degrees in electrical engineering from Moscow Power Engineering Institute, Moscow, Russia, in 2014 and 2016, respectively, and the Ph.D. degree in engineering systems from the Skolkovo Institute of Science and Technology, Moscow, in 2020. From 2021 to 2024, he was a Research Associate with The University of Manchester, Manchester, U.K. He is currently a Research Associate of AI and analytics for electricity markets with the Dyson School of Design Engineering, Imperial College London, London, U.K. His research interests include mathematical optimisation, game theory, electricity markets, energy economics, data valuation and data marketplaces, and power system flexibility.

Robin Preece (Senior Member, IEEE) received the B.Eng. and Ph.D. degrees from The University of Manchester, Manchester, U.K. He is currently a Professor of future power systems with the Department of Electrical and Electronic Engineering, The University of Manchester, where he has been an Academic, since 2014. His research focuses on stability and operation of future power systems.

Rodrigo Moreno (Member, IEEE) received the B.Sc. and M.Sc. degrees from the Pontificia Universidad Catolica de Chile, Santiago, Chile, and the Ph.D. degree from the Imperial College, London, U.K. He is currently an Assistant Professor with the University of Chile, Santiago. His research interests include power system optimization, reliability and economics, renewable energy, and smart grids.

Eduardo A. Martinez Ceseña (Member, IEEE) received the M.Sc. degree in power systems from the Instituto Tecnológico de Morelia, Morelia, Mexico, and the Ph.D. degree from The University of Manchester (UoM), Manchester, U.K. He is currently a Senior Lecturer or Associate Professor of multi-energy systems with the Department of Electrical and Electronic Engineering, UoM. His research interests include planning and design of resilient multi-energy systems and integrated electricity-heat-gas networks, power system economics, real options theory, and optimization techniques.